

Chapter 8. Vacuum

Terry Anderson and Evan Malone

8.1. Design Overview

The Proton Driver Ring Vacuum System is a 711-m continuous vacuum chamber composed of magnets, short sections of tubing, bellows, ion pumps, valves, and instrumentation. The system is divided into twenty (20) sectors, eighteen (18) ring sectors and two (2) transfer lines. The complete Proton Driver Ring layout is shown in Figure 8.1 and a detailed layout of typical sectors is shown in Figure 8.2. Table 8.1 shows the primary system design parameters used as the basis for this description.

Table 8.1. Vacuum System Design Parameters

Average Pressure Range	10^{-7} to 5×10^{-8} Torr
Total System Length	711 m
Vacuum Sector Lengths	69.3 m, 41.7 m, 36.7 m, and 29 m.
Vacuum Aperture	5" \times 9"
Primary Pump Type	Ion Pump, 800 l/s.
Roughing Pump Type	Turbo Molecular (500 l/s), w/10 CFM Dry Backing Pump.
Sector Pump-down Time	12 hr to rough; 72 hr bake-out to high vacuum.
Vacuum Gauging	Pirani, Ion Gauge and Ion Pump read-back.
Beam Tube Material	Straight Sections and Magnets without eddy current heating: Stainless Steel Magnets with eddy current heating: Titanium.
Vacuum Interface Type	Flanged w/bellows.
Special Considerations	Dipoles and Quadrupoles will be of a vacuum canned design (core and coils will be in the vacuum space).
Bake-out System	Magnet vacuum chambers will have low temperature (<150 C) bake-out capability.

The primary vacuum system operating parameter for the Proton Driver is the base pressure, 10^{-7} Torr. In typical accelerator vacuum systems this is relatively easy to obtain. Most systems are limited by the aperture conductance and the specific out-gassing rate of the chamber walls. In typical systems at 10^{-7} Torr these limitations are easily overcome by reasonable spacing of relatively small pumps. Pump down times are generally on the order of several hours to one day and are for the most part determined by the time it takes for the specific out-gassing rate to reach 10^{-10} to 10^{-11} Torr-l/s-cm². These rates are the lower limits of metals with many monolayers of water molecules adsorbed on the surface and only improve over a long time or by baking the system. Although the Proton Driver is not limited by conductance issues it is limited by the amount of pumping available and the specific out-gassing rate due to the extremely large amount of surface area in the canned

magnets and the high out-gassing of the coil assemblies. In order for the Proton Driver to reach 10^{-7} Torr it is necessary for the out-gassing rates of the magnet laminations and the coil assemblies not to exceed 5×10^{-13} and 10^{-9} Torr-l/s-cm² respectively. This can only be achieved by fabricating all components that make up the vacuum system using ultra-high vacuum (UHV) practices and incorporating in a (relatively) low temperature bake-out system.

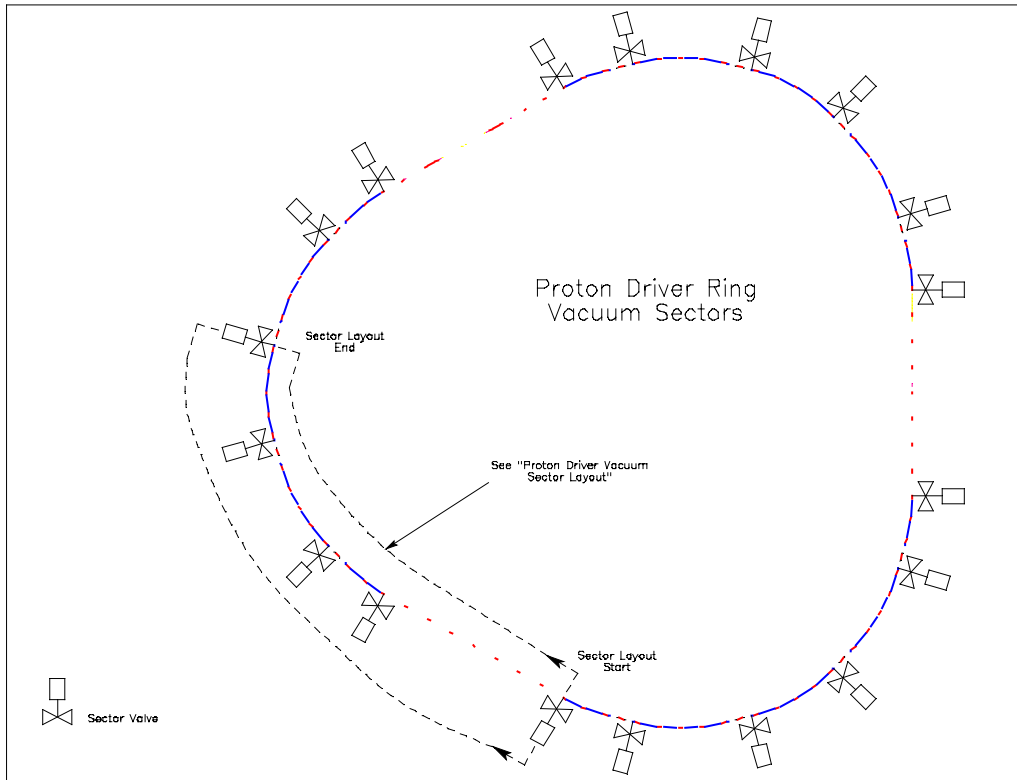


Figure 8.1. Proton Driver Ring Vacuum Sector

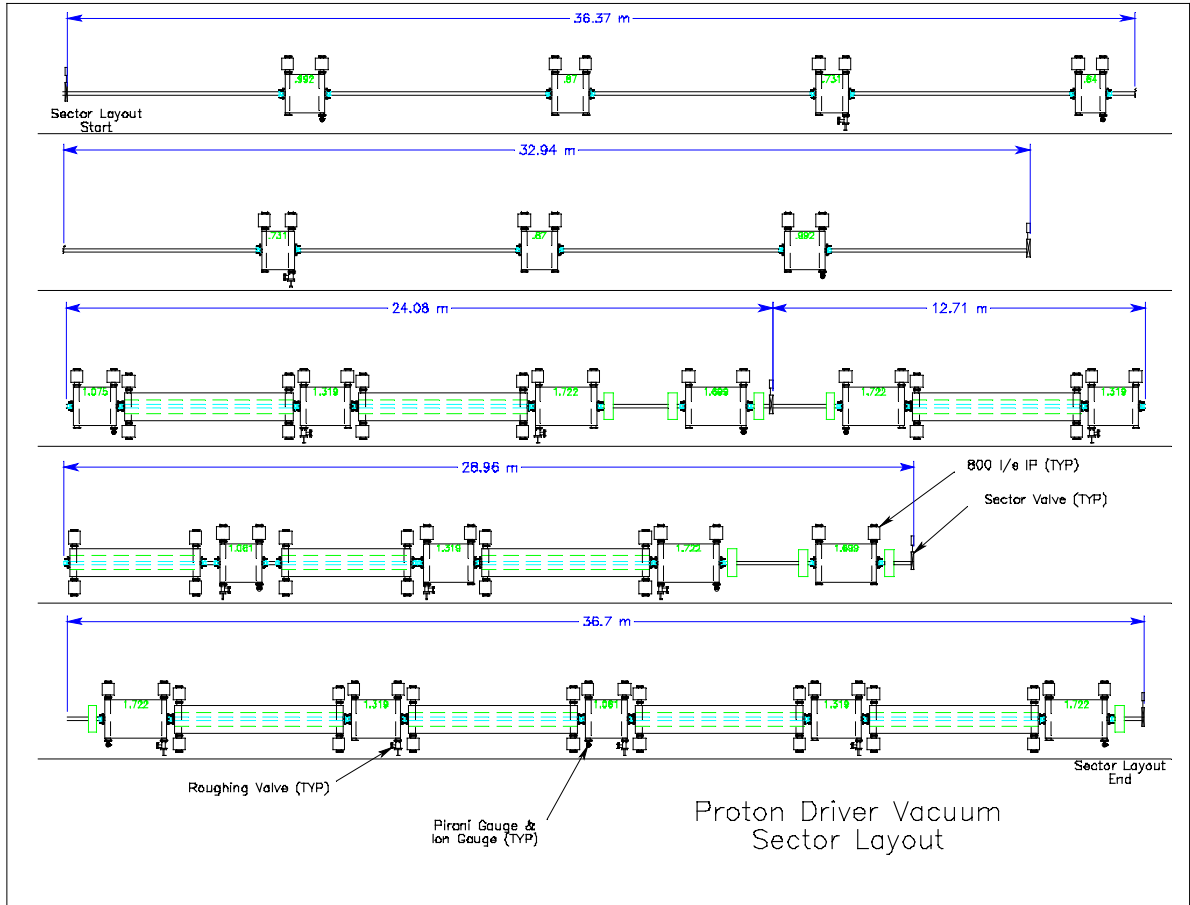


Figure 8.2. Proton Driver Vacuum Sector Layout

8.2. System Components

The vacuum system components for the Proton Driver are, with the exception of the magnets and bellows, fairly standard high to ultra high vacuum components. The magnets are discussed in Section 8.3 below and the bellows are similar to those used in the Fermilab Recycler. The concept is a round, stainless steel, formed bellow and tube section with the basic aperture cross-section. The tube sections extend into the bellow space and a thin (0.005-inch) metallic foil is allowed to slide over the two tube ends to provide rf shielding. The basic vacuum interface is shown in Figure 8.3.

The interface design uses EVAC style ISO NW 250 flanges with chain style clamps. This reduces the amount of space needed between magnet ends, as opposed to Conflat style flanges, and also reduces the exposure time during maintenance operations, thereby contributing to radiation ALARA compliance. Straight sections will be made of stainless steel tubing with a cross-section conforming to the basic aperture. Each end of the straight section will have a bellows and flange. The current design has no vacuum ports or components on the vacuum chamber in the straight sections. All ports and components are on the magnets.

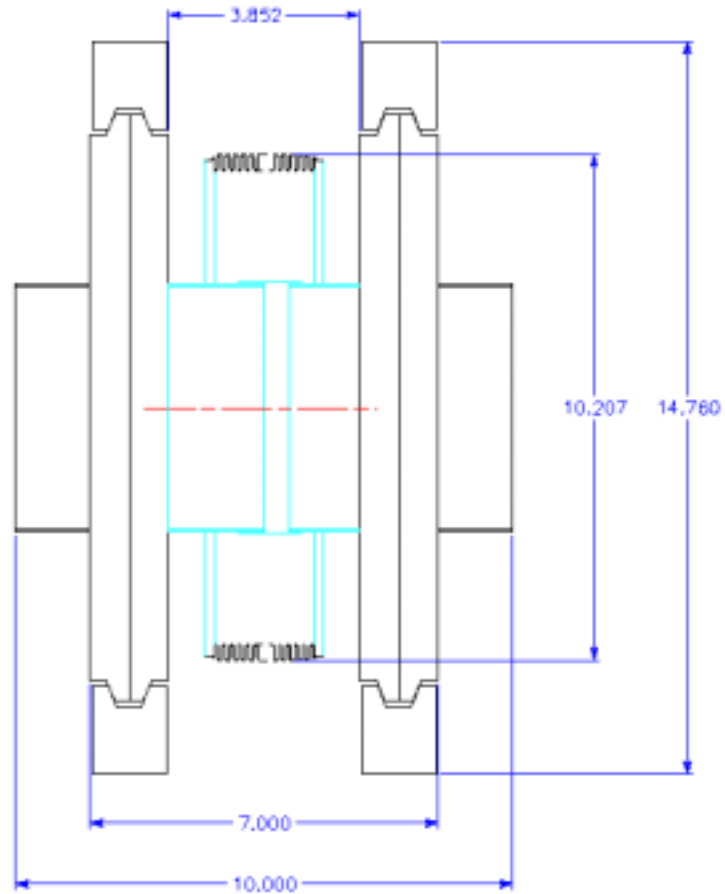


Figure 8.3. Proton Driver Quad/Dipole Interface with Bellows

The remaining basic permanently installed components are: 800 l/s ion pumps, 6 inch roughing valves, Pirani gauges, ion gauges, 10 inch rf shielded sector valves, and the control and read-back systems for each component. The basic vacuum sector configurations are shown in Figure 8.2. Portable turbo molecular roughing carts will attach to the roughing valves for pump down. Other components and systems used in the vacuum system are temperature sensors and controllers for magnet bake-out, a compressed air system for sector valve operation, and stands for valves, chambers, and ion pumps.

8.3. Magnet Vacuum

The proposed magnet design for the Proton Driver is a canned magnet with coils and core contained within the vacuum shell. With this type of design the dominant gas load for the vacuum system comes from the core and the coils, the core due to the large surface area of the laminations and the coil due to the higher out-gassing rate of the insulating material. The design is based on the out-gassing rates shown in Table 8.2.

Table 8.2. Outgassing rates

	Out Gassing Rate (Torr-l/s-cm ²)
Skin	5×10^{-13}
Laminations	5×10^{-13}
Coil	1×10^{-9}

The surface areas for the largest of the Proton Driver magnets are shown in Table 8.3 along with the calculated pressure at the pump, assuming multiple 800 l/s ion pumps for each magnet. The magnet also contains a beam tube, but the gas load contribution from the tube is negligible. A discussion of the beam tube is in Section 8.4 below.

Table 8.3. Vacuum Design Numbers for Proton Driver Magnets

Magnet	Surface Area (cm ²)			Total Gas Load (Torr-l/s)	Pump Speed (l/s)	Pump Pressure (Torr)
	Skin	Laminations	Coil			
5.25 m Dipole	2.77×10^5	2.80×10^8	1.71×10^5	3.11×10^{-4}	3200	9.71×10^{-8}
3.93 m Dipole	2.07×10^5	2.10×10^8	1.28×10^5	2.33×10^{-4}	3200	7.28×10^{-8}
1.72 m Quad	9.73×10^4	1.05×10^8	6.29×10^4	1.15×10^{-4}	1600	7.21×10^{-8}
1.70 m Quad	9.62×10^4	1.04×10^8	6.22×10^4	1.14×10^{-4}	1600	7.14×10^{-8}
1.32 m Quad	7.47×10^4	8.06×10^7	4.83×10^4	8.86×10^{-5}	1600	5.54×10^{-8}
1.06 m Quad	6.00×10^4	6.47×10^7	3.88×10^4	7.12×10^{-5}	1600	4.45×10^{-8}

To achieve the out-gassing rates in Tables 8.2 and 8.3 the magnet assembly needs to be constructed using UHV practices. Steel components will need to be hydrogen degassed prior to assembly and special care taken to insure that all materials in the assembly are free of contaminants such as oils and greases. All materials must be capable of surviving repeated low temperature (150° C) bakes.

From a vacuum standpoint, the coil pack will be especially challenging. The conductor that will be used is a square copper stranded conductor. The strands are wrapped around a stainless steel cooling tube for the LCW cooling water. In order to minimize the gas load due to this assembly, the coil pack will need to be vacuum impregnated with a low out-gassing epoxy type material (preferably polyimide) and then wrapped with a polyimide film. The film must have a near 100% bond to the coil pack to prevent local delaminating that would create unacceptable virtual leaks. The basic concept is to create a low out-

gassing surface that atmospheric gasses will not penetrate to any great degree when the system is let up to atmospheric pressure. Some R&D work still remains to be done with respect to the coil pack design, but the general consensus is that an out-gassing rate of 10^{-9} Torr-l/s-cm² is achievable. With considerably more R&D work it is conceivable that the outgassing rate could be reduced by an additional order of magnitude, thereby giving a factor of two decrease in operating pressure.

8.4. Beam Tubes

Besides providing an unobstructed path for the beam, the beam pipe must also control the resistive wall impedance (shielding). Typically, a simple stainless steel pipe serves both purposes, but for the Proton Driver a traditional approach is problematic. The large transverse emittance of the beam requires a large chamber aperture, and therefore large expensive magnets to provide required magnetic field properties over such a large area. Thick chamber walls would be required to support the pressure differential, but such walls would increase the magnet size and cost by consuming aperture. The 15 Hz cycling of the machine would drive immense eddy currents in a metallic chamber inside of the dipole magnets, wasting power and necessitating cooling and field correction. Nevertheless some metal is required to provide adequate shielding. The design chosen attempts to circumvent many of these constraints by segregating the functions of the beam pipe into physically distinct components. The eddy currents are minimized and the aperture maximized by moving the "vacuum skin" to the outside of the magnets. Only the amount of metal required for shielding need be placed inside.

Two methods of shielding the beam are under consideration. The preferred method nearly eliminates eddy currents by dividing the metal shield into parallel, longitudinal conductors capacitively coupled at one end to the next section of beam tube, and in electrical contact at the other end with the previous section of beam tube. This is shown in Figure 8.4. The shield thus acts as a high pass filter. The capacitors act as short circuits for the high frequency beam image currents, but present an open circuit to the 15 Hz eddy currents, confining them to within individual stripes. Because the currents circulate only within a stripe, magnetic fields of neighboring stripes largely cancel each other and Lorentz forces act only within stripes, not between them. This shielding concept was pioneered at the Rutherford Laboratory ISIS spallation source, and has been highly successful [1]. The proposed implementation of this concept for the Proton Driver was conceived of by Bruno Zotter of CERN [2].

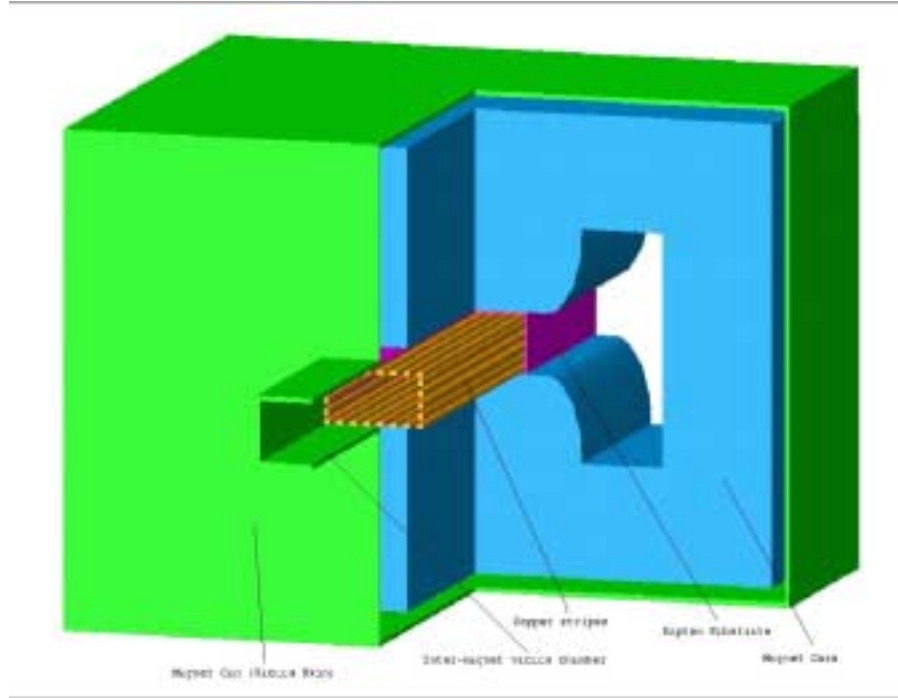


Figure 8.4. Corner Section of Canned Dipole (Striped Shield)

In the Zotter shield, closely spaced copper strips, ~ 0.1 mm thick and 4 mm wide, would be attached to a thin (~ 1 mm) insulating substrate (e.g. Kapton) of rectangular cross section. This would surround the beam supported by adhesive bonds to the magnet pole tips. The cross section of the shield and substrate would need to be contoured to accommodate the reduced diagonal dimensions available within the quadrupoles and sextupoles. There are, however, concerns about the transverse wall impedance that may result from this type of shield. Previous laboratory measurements [3] indicate strips have much larger transverse impedance than that of a uniform metallic coating. Possible resonances that may result from the gaps between strips are also concerns. [11] Currently there is no consensus of theoretical analysis on this type of shield. Technical measures, such as adding circumferential strips insulated from the longitudinal strips [4], may be able to resolve some of these concerns, but further investigation is warranted.

A second shield concept has been examined as an alternative to the Zotter design. A tube of rectangular cross-section, roughly $23\text{ cm} \times 13\text{ cm}$, made of an electrically resistive metal alloy, ~ 0.13 mm thick, surrounds the beam inside the magnets. The tube is perforated to permit evacuation of its interior and the perforations are randomly located to prevent electromagnetic resonances. This is shown in Figure 8.5.

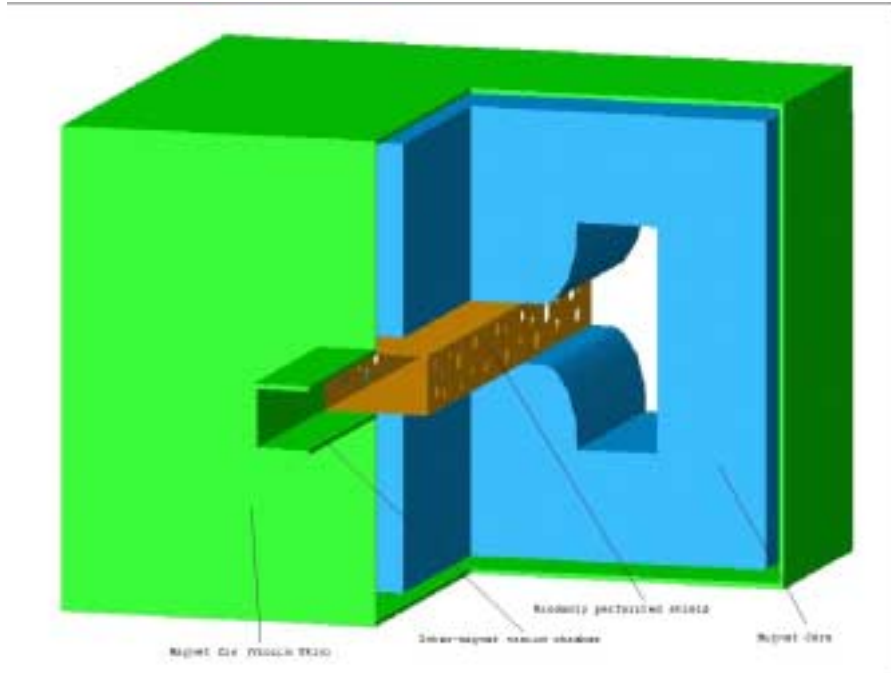


Figure 8.5. Corner section of Canned Dipole (Perforated Tubular Shield)

As in the first concept, the cross-section would need to be contoured within the quadrupoles and sextupoles to accommodate the reduced dimension. The associated resistive wall impedance has not been definitively determined and warrants further investigation. This design must cope with significant eddy currents and their consequences (Lorentz forces, resistive heating, and magnetic field distortions). Due to the thinness of the shield material a means of supporting it against the 15 Hz Lorentz forces without significantly impeding heat transfer will need to be developed. Simulations have shown that 1.2 kW/m or more of eddy current heat can be radiatively transferred to the dipole magnet core without thermal damage to the shield, the core, or the conductor insulation (Figure. 8.6).

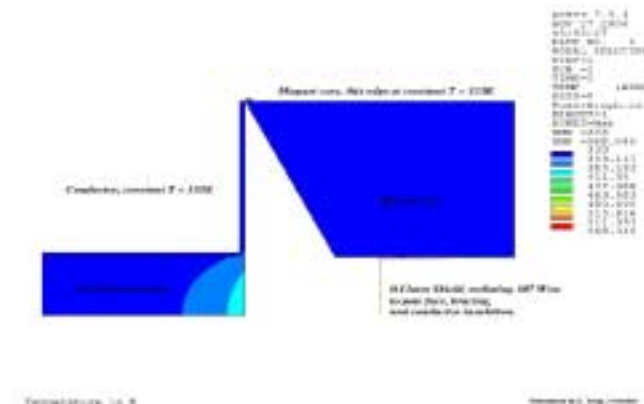


Figure 8.6. FEM of Radiative Heat Transfer from Tubular Shield to Dipole Core

The resulting non-uniform thermal expansion of the magnet core (Figure 8.7) results in substantially less pole face distortion than the 0.13 mm "maximum deviation from planarity" criterion employed during the conceptual design [5].



Figure 8.7. Plot of Vertical Component of Dipole Pole Face Thermal Displacement

A passive scheme for compensating the sextupole magnetic field resulting from the eddy currents has been investigated [6, 7] and seems very promising. Despite the additional complexity of the compensation system, and the significant eddy current heating, this shielding design is considered to be a practical alternative to the Zotter shield.

It is useful to compare the consequences of the two proposed shield designs. Let $I_{beam,RMS}$ be the RMS beam current, ω the beam angular circulation frequency, $B(t)$ the dipole magnetic field, and $B'(t)$ its time derivative. Using these variables, one can calculate I_{eddy} , the induced eddy current, F_{Lor}/l , the total Lorentz force per unit length, P_{eddy}/l , the total eddy current resistive dissipation per unit length, P_{image}/l , the RMS beam image current resistive dissipation per unit length, and d_s , the longitudinal "shielding condition" shield thickness.

The formulae for each design are given in Table 8.4. Using the operating parameters from Table 8.5, results for specific implementations of these two shield designs are given in Table 8.6. It is assumed that for shields in quadrupoles and sextupoles the eddy currents and their consequences would be reduced by at least one order of magnitude; thus the emphasis is on the dipole design.

Table 8.4. Shield Design Equations

<p>RECTANGULAR TUBE width: $2a$, meters height: $2b$, meters thickness: d, meters shortest distance shield to pole: h, meters mag permeability: $\mu = \mu_r \mu_0$, Henry per m electrical resistivity: ρ, Ohm-meters</p>	<p>LONGITUDINAL STRIPES stripe width: $2w$, meters stripe thickness: d, meters hor stripes (top + bottom surfaces): N_H vertical stripes (left + right surfaces): N_V shortest distance shield to pole: h, meters mag permeability: $\mu = \mu_r \mu_0$, Henry per m electrical resistivity: ρ, Ohm-meters</p>
<p>$I_{eddy}(t) = B'(t) a d (a + 2b)/\rho$ Amps</p>	<p>$I_{eddy}(t) = B'(t) d w^2/2\rho$ Amps, inside one horizontal stripe</p>
	<p>$I_{eddy}(t) = B'(t) w d^2 /2\rho$ Amps, inside one vertical stripe</p>
<p>$F_{Lor}/l = B(t)I_{eddy}(t)$ $= B(t)B'(t) a d (a+2b)/\rho$ N/m</p>	<p>$F_{Lor}/l = B(t)I_{eddy}(t)$ N/m, acting only within a stripe</p>
<p>$P_{eddy}/l = 4B'(t)^2 a^2 d (a/3+b)/\rho$ Watts/m</p>	<p>$P_{eddy}/l = 2B'(t)^2 wd (N_H w^2 + N_V d^2)/3\rho$ Watts/m.</p>
<p>$P_{image}/l \approx (I_{beam,RMS})^2 \rho /2d/(2a + 2b)$ Watts/m</p>	<p>$P_{image}/l \approx (I_{beam,RMS})^2 \rho /2wd/(N_H + N_V)$ Watts/m</p>
<p>$d_s \gg \rho/\mu wh$ m</p>	<p>$d_s \gg \rho/\mu wh$ m</p>

Table 8.5. Relevant Proton Driver operating parameters

	Phase 1, Stage 1	Phase 1, Stage 2
ω (at injection)	1.88×10^6 radian/s	1.88×10^6 radian/s
$B'(t)_{RMS}$	35 T/s	47 T/s
$Max(B(t)B'(t))$	34 T ² /s	61 T ² /s
$I_{beam,RMS}$	2.69 A	7.12 A

Table 8.6. Shield Design Results

	RECTANGULAR TUBE (Inconel alloy 718) $2a = 0.2286$ meters $2b = 0.127$ meters $d = 1.27 \times 10^{-4}$ meters $h = 1 \times 10^{-3}$ meters $\mu = 1.002 \mu_0$ Henry per m $\rho = 121 \times 10^{-8}$ Ohm-meters		LONGITUDINAL STRIPES (Oxygen Free Copper) $2w = 4 \times 10^{-3}$ meters $d = 1 \times 10^{-4}$ meters $N_H = 100$ (2 sheets of 50) $N_V = 54$ (2 sheets of 27) $h = 1 \times 10^{-3}$ meters $\mu = 1.000 \mu_0$ Henry per meter $\rho = 1.71 \times 10^{-8}$ Ohm-meters	
	Stage 1	Stage 2	Stage 1	Stage 2
$RMS(I_{eddy})^1$	101 A	136 A	1.64 A (in one horizontal stripe)	2.20 A (in 1 one horizontal stripe)
			40.9 mA (in one vertical stripe)	55.0 mA (in one vertical stripe)
$MAX(F_{Lor}/l)^1$	98.4 N/m	177 N/m	1.59 N/m (in one horizontal stripe)	2.85 N/m (in one horizontal stripe)
			39.8 mN/m (in one vertical stripe)	71.3 mN/m (in one vertical stripe)
$RMS(P_{eddy}/l)$	683 W/m	1230 W/m	30.6 W/m	55.1 W/m
$RMS(P_{image}/l)$	96.9 mW/m	679 mW/m	1.00 mW/m	7.04 mW/m
d/d_s (longitudinal, at injection)	0.25		13.8	

In the course of the conceptual design of the Proton Driver, several additional vacuum chamber designs were considered. Each of the designs involved some significant drawback that made it inferior, at this stage, to the design selected. A brief description of these designs and the decisive issues associated with them follows. More detailed technical descriptions of the R&D work on those designs will be available in Fermilab technical notes.

The first design investigated was a metallic vacuum chamber $22.86 \text{ cm} \times 12.7 \text{ cm}$ (9 in \times 5 in) elliptical cross section, made of 1.27 mm (50 mils) thick Inconel alloy 718 (Figure. 8.8). The significant distortion of the chamber wall under vacuum required that the tube be

¹ Note: eddy currents and Lorentz forces for the striped shield are confined to the interior of each stripe. There are essentially no inter-stripe forces, and magnetic fields generated by eddy currents in one stripe are essentially cancelled by fields from neighboring stripes.

initially formed to a less eccentric cross-section than desired for the final chamber. The chamber would need to be built inside of the dipole magnets. Despite being constructed of thin, highly electrically resistive alloy, this chamber would experience eddy currents of 1370 A inside the dipole magnets. This would result in very large and difficult to correct sextupole (and higher order) fields, and nearly 8500 W/m of eddy current heating. The design therefore would require the passive sextupole compensation system mentioned above, as well as an active cooling system. Significant effort was expended on development and processing of thermally conducting, electrically insulating epoxy materials to increase thermal contact between the cooling pipes and the chamber, and promising results were obtained. However, the longevity of these materials in service, as well as the significant quantity of power wasted, the large sextupole fields, and the difficulty of building and maintaining the system make it undesirable.

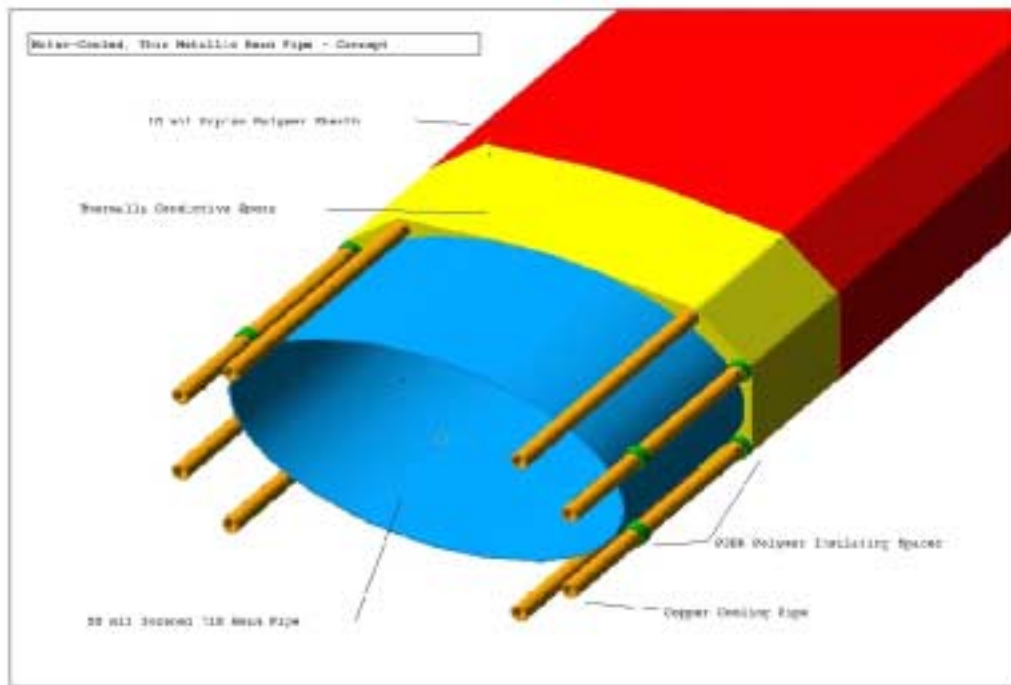


Figure 8.8. Water-cooled Vacuum Chamber Design

A second design investigated was an extrapolation of a vacuum chamber design used in the DESY III accelerator [8]. The particular implementation studied involved a metallic vacuum chamber of 22.86 cm × 12.7 cm (9 in × 5 in) elliptical cross section, made of 0.127 mm (5 mils) thick Inconel alloy 718. Reinforcing ribs of 1 mm thick alloy 718 were brazed to the outside, 75 ribs per meter of tube, to support it against atmospheric pressure. In practice, obtaining a high enough braze quality without distorting such flimsy material proved exceedingly difficult (Figure 8.9). In addition, though the eddy currents and their effects are reduced by a factor of ten from the first design described, they are still quite large. Sextupole compensation would be required, the chamber and adjacent materials inside of the dipole magnets would reach high temperatures (300° C) without active cooling, and any significant deviation of the supporting ribs from parallelism with the

magnetic fields would result in catastrophic eddy currents, probably destroying the chamber. For these reasons, this design was rejected.



Figure 8.9. Photograph of Unsuccessful Prototype of Rib-Reinforced Vacuum Chamber

A third design is based on metal foil lined, fiber-reinforced epoxy chambers built for the CERN SPS interaction region during the mid-1980's [9]. Such chambers are conceptually similar to chambers of ceramic, with an insulating external structure surrounding/supporting a metallic shield of some sort. In particular, to manufacture the composite vacuum chamber, a metal tool form of the desired cross-section would be wrapped with the desired shield material, for instance a continuous Titanium alloy foil, or longitudinal copper stripes on a Kapton polymer backing. A ceramic fiber impregnated with a bismaleimide resin would then be wound over the tool and the shield material to build up the desired thickness. The resin is cured and metal flanges would be bonded to the ends. Composite chambers can be nearly as strong and stiff as ceramic, but are less brittle, and so can be made slightly thinner. Composite chambers also can be manufactured in single units of 6 m or more in length, can be curved, and are significantly cheaper per unit. However, the durability of epoxy composite materials in accelerator service conditions of thermal and mechanical cycling, radiation, and high humidity, and the vacuum out-gassing and gas permeability of such materials need further investigation. Fermilab lacks the equipment to manufacture high-performance, filament wound composite materials, and the high cost of outsourcing the work (> K\$ 100) prevented further investigation of the design at this time. Composite chambers are considered to be very promising and worthy of further R&D.

8.5. Vacuum Performance

As stated earlier, the primary vacuum system operating parameter for the Proton Driver is the 10^{-7} Torr base pressure. Because of the need to have as low as possible out-gassing rates, this can only be achieved after a low temperature bake-out for at least seventy-two (72) hours. The vacuum sectors have been made sufficiently short to minimize the number of turbo carts and to create manageable sections for bake-out operations. The longest sector is the 69.3 m straight section containing seven (7) quadrupoles. The most difficult sector to pump down is the 36.7 m arc sector that contains five (5) quadrupoles and four (4) dipoles. The performance curves for the straight section and the arc sector are shown in Figures 8.10 and 8.11, respectively.

In both charts the top curve (black) is the sector pressure profile during rough down at the end of the bake-out. The middle curve (purple) is the sector pressure profile after starting the ion pumps on the quads that the turbo carts are attached to. The bottom curve (orange) is the sector pressure profile after all ion pumps have been started and the system has cooled down to ambient conditions. In both cases the final average steady state pressure is less than 10^{-7} Torr. In the arc sector, at the center of the dipoles, the pressure does peak at 1.24×10^{-7} Torr but the average is still less than 10^{-7} Torr.

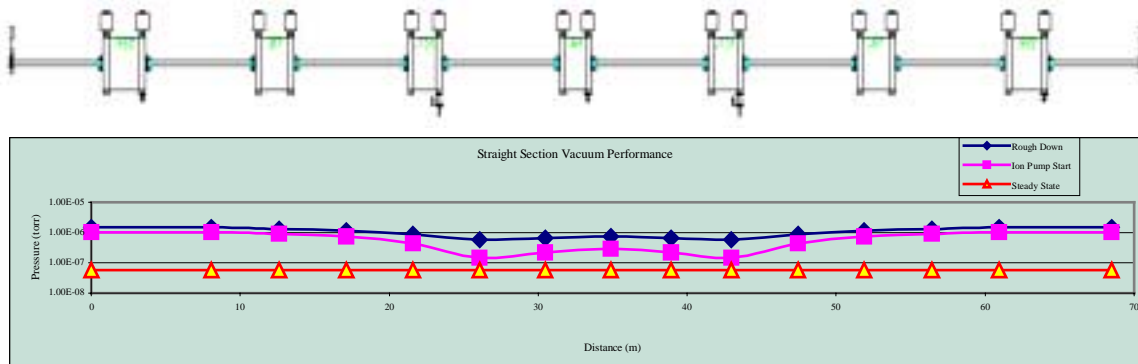


Figure 8.10. Straight Section Vacuum Performance

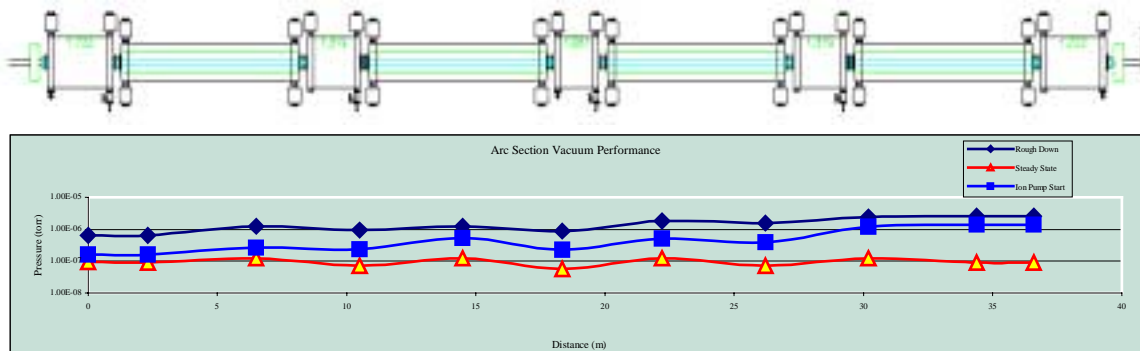


Figure 8.11. Arc Section Vacuum Performance

8.6. R&D Efforts

The main remaining vacuum issue is the outgassing rate of the coil assembly. It is believed that we can obtain a rate of 10^{-9} Torr-l/s-cm², but this needs to be verified experimentally. With further R&D to improve this rate it should be possible to realize a factor of two (2) or better decrease in the ultimate pressure, putting the vacuum level comfortably in the mid to low 10^{-8} Torr range.

The highest priority for research and development related to the magnet beam tubes for the Proton Driver is to establish a solid and experimentally verified understanding of the minimum beam shielding requirements for tolerable resistive wall impedance. If discontinuous shield designs (capacitively coupled stripes) provide sufficient shielding, then eddy-currents and all of their consequences are practically eliminated. Magnetic field distortion compensation becomes unnecessary. Power dissipation is minimal, and thus heat transfer, material temperature limits, and thermal stresses are of little concern and Lorentz forces are small. If a continuous shield is required, then awareness and use of the minimum shield thickness permits the minimization of eddy-currents and their consequences.

During the conceptual design of the Proton Driver, vacuum chambers made of fiber-reinforced epoxy with a continuous metal foil lining were investigated [10]. This design was extrapolated from composite chambers designed for the CERN SPS interaction region, which had significantly different design constraints [9]. The lining is intended to reduce the permeation of gases through the composite material and to provide shielding for the beam. There is consensus that this design is worthy of further investigation and prototyping, as it could provide a very thin chamber with significant cost and manufacturing advantages. There is the potential for a significant break through for the Proton Driver. Successful implementation of this design would significantly reduce the pumping and cost requirements of the vacuum system. In addition the magnet costs would be reduced due to elimination of the canned magnet design.

The following is a list of R&D activities that should be undertaken to address the issues and opportunities discussed above.

For verification of coil out-gassing rates:

- 1) Out-gassing tests on various coil coatings and configurations.

For understanding of the minimum shielding requirement:

- 1) Additional theoretical investigation of the minimum beam-shielding requirement and of the longitudinal and transverse resistive wall impedance of discontinuous (striped) shielding.
- 2) Laboratory and accelerator tests of resistive wall impedances of thin, metallic tubular and striped shield designs.

For evaluation of fiber-reinforced epoxy composite vacuum chambers:

- 1) Tests of vacuum out-gassing and permeability of gasses through candidate materials.
- 2) Evaluation of processes/coatings/linings to enhance vacuum properties if necessary.
- 3) Tests of thermal and mechanical properties of candidate materials.
- 4) Tests of effects of radiation exposure on vacuum and mechanical properties of candidate materials (service lifetime).
- 5) Small scale prototyping and testing of tubes with various interface (flange) and shielding (Kapton with copper stripes, Ti alloy foil liner, etc.) designs.
- 6) Prototyping and in-accelerator testing of best designs to establish manufacturing process and validate design.

Assuming that the minimum shielding requirement is well understood, and that the two shielding methods described for the proposed "canned magnet" vacuum system are still feasible in light of that understanding, practical implementations of these two designs will depend upon engineering solutions to several outstanding problems. The following is the R&D effort that will need to be conducted based on the outcome of the beam shielding assessment.

For the perforated, thin-wall tubular shield in "canned magnet" vacuum system:

- 1) Development of manufacturing process to produce randomly perforated thin-wall tubing.
- 2) Development of mechanical support structure to reinforce thin-wall shield against Lorentz forces without impeding heat flow from shield to surroundings.
- 3) Prototyping of eddy-current magnetic field passive compensation system.
- 4) In-magnet tests (comparable dB/dt to Proton Driver) to validate shield and eddy-current magnetic field compensation system designs.

For the striped shield in "canned magnet" vacuum system:

- 1) Evaluation of mechanical, vacuum and radiation properties of candidate substrate materials for metallic stripe shield designs.
- 2) Evaluation of mechanical, vacuum, and radiation properties of adhesive or other stripe-to-substrate bonding methods and substrate-to-magnet pole bonding methods.
- 3) Design and testing of capacitive interconnection of stripes to intermagnet vacuum chamber.

References

- [1] Rees, G.H., "Aspects of Beam Stability at ISIS," in: Workshop on Instabilities of High Intensity Hadron Beams in Rings, Upton, NY, USA, June 28 - July 1, 1999, pp. 17 – 21
- [2] See Ch. 4, sections 4.2.1-4.2.2 of this report
- [3] Walling, L.S., et. al., "Transmission-Line Impedance Measurements for an Advanced Hadron Facility," Nuclear Instruments and Methods in Physics Research, North-Holland, Amsterdam, A281 (1989), pp. 433-447
- [4] Harvey, A., "Tailored Vacuum Chambers for AC Magnets," IEEE Transactions on Nuclear Science, V. NS-32, Number 5, Oct. 1985, pp. 3815 – 3817
- [5] Mills, F., personal communication, ~9/1999
- [6] Danby, G., et. al., "Description of New Vacuum Chamber Correction Concept," Brookhaven National Laboratory, BNL41856, 1989
- [7] See discussion in Chapter 6 of this report
- [8] Kouptsidis, J., et. al., "A Novel Fabrication Technique for Thin Metallic Vacuum Chambers with Low Eddy Current Losses," IEEE Transactions on Nuclear Science, V. NS-32, Number 5, Oct. 1985, pp. 3584-3586
- [9] Engelmann, M., et. al., "Vacuum Chambers in Composite Material," Journal of Vacuum Science and Technology A, 5, Jul/Aug 1987, pp. 2337-2341
- [10] Anderson, T., Malone, E., "Fermilab Proton Driver: R&D Effort for Composite Vacuum Chamber," PDF file on Proton Driver Website, <http://www-bd.fnal.gov/pdriver/systems/CompositeTubeInfo.pdf>
- [11] W. Chou and T. Barts, "Impedance of a Perforated Liner and Its Impact on the SSC Collider," Proc. of the 1993 IEEE Particle Accelerator Conference, May 17-20, Washington, D.C., p. 3444.